

Diagnostic Testing of a Glow Plasma Discharge Tube

by

Juan Marquez

Submitted in Partial Fulfillment of the
Requirements for the Degree

Bachelor of Arts

Supervised by
Dr. Daniel Borrero-Echeverry

Department of Physics

Willamette University, College of Liberal Arts
Salem, Oregon

2019

Presentations and Publications

- May, 2018. Willamette University ATEP Presentations. Period Doubling in Plasma. Oral Presentation.
- December, 2018. Physics 495 Research Seminar I. Period Doubling in Plasma. Oral Presentation.
- April, 2019. Student Scholarship Recognition Day (SSRD) Presentation Period Doubling in Plasma. Oral Presentation.
- May, 2019. Willamette/Linfield/Pacific Poster Presentation. Diagnostic Testing using a Glow Discharge Plasma Tube. Poster Presentation.

Acknowledgments

I'd like to thank Dr. Daniel Borrero for guiding my research experience and answering my questions. I'd also like to thank Dr. Rick Watkins for answering my coding and formatting questions, and helping me with my research. I'd also like to thank Jonathan F. Reichert Foundation for supporting my research.

Abstract

General Abstract

Plasma is the fourth state of matter, and despite decades of study, there are still many unanswered questions. A plasma tube is a great object to create and do test on plasma. Our project was to assemble the glow discharge plasma tube and run diagnostic test and report them in this thesis.

Technical Abstract

The glow discharge plasma tube is a great tool for undergraduate students to conduct their own research. We endeavored to understand the reason behind why plasma waves inside a discharge tube undergo period double bifurcations and eventually follow Feigenbaum's route to chaos. However, diagnostic testing first took place because it is the first time Willamette University has established a DC glow discharge apparatus. We used our plasma tube setup to measure the Paschen curve, and document the plasma's current-voltage curve using a Langmuir probe to estimate the electron temperature. However, during the measurements of the current-voltage curve, there were only 2 points recorded near the floating potential, resulting in a questionable electron voltage of 2.82 eV. We also attempted to measure the electron temperature using spectral lines of nitrogen, but values such as quantum degeneracy value are not known for nitrogen because it is unknown if we are using atomic or molecular nitrogen.

Table of Contents

| | |
|---|------------|
| Acknowledgments | iii |
| Abstract | iv |
| List of Tables | vi |
| List of Figures | vii |
| 1 Introduction | 1 |
| 1.1 Plasma | 1 |
| 1.2 Plasma waves | 2 |
| 2 Background Information | 4 |
| 2.1 Paschen Law | 5 |
| 2.2 Probe Theory | 9 |
| 2.3 Period Doubling | 13 |
| 3 Diagnostic Tests | 19 |
| 3.1 Measuring the $I - V$ curve | 19 |
| 3.2 Obtaining the Paschen Curve | 24 |
| 3.3 Spectroscopy | 26 |
| 4 Results | 29 |
| 5 Discussion | 31 |
| Bibliography | 34 |

List of Tables

- 1 A table of all the wavelengths present in the nitrogen-based plasma. The dashed lines represent data could not be found for those specific wavelengths. The *R*'s next to the wavelengths means that the wavelength is the Ritz wavelength, which are wavelengths calculated from energy level differences. For all of the wavelengths, we had to take the closest wavelengths listed on the NIST website. . . . 32

List of Figures

| | | |
|-----|--|----|
| 1.1 | A picture of standing striation waves near the positively charged electrode with a probe inserted in the tube. | 3 |
| 2.1 | The volume a single particle takes up as it moves through the tube before it collides. Adapted from Ref. [6]. | 7 |
| 2.2 | A specific section of the tube where the electrons start at x_0 and travel a distance Δ . It also shows some of the electrons are unable to reach the final distance $x_0 + \Delta$ as they collide prematurely. Adapted from Ref. [6]. | 8 |
| 2.3 | Paschen's Law allows us to calculate the V_B as a function of electrode spacing and pressure. The actual points represents the data taken and the curve represents the best-curve fit. We worked with the parameters to make the best fit possible, and the graph is the best fit. | 10 |
| 2.4 | A Langmuir probe with a tungsten tip with various parts annotated. | 11 |
| 2.5 | a system in which undergoes a Hopf bifurcation which make oscillatory and then undergoes a period doubling bifurcation. After the system undergoes period doubling bifuraction, two frequencies now exist. | 14 |
| 2.6 | An example showing a qualitative bifurcation. a) for small masses the beam can support. b) for large masses the beam cannot support and buckles as a result. | 15 |
| 2.7 | A pitchfork bifurcation that splits into two stable and one unstable solutions after undergoing a change at $r = 0$. A solid line represents a stable solution while a dashed line represents an unstable solution. | 16 |

- 2.8 A system undergoing a Hopf bifurcation at r_1 and a period doubling bifurcation at r_2 . Once the system goes from a time-independent to a time-dependent system at r_1 , the system oscillates back and forth between points, and the amplitude continues to increase as r increases. While it starts to look less sinusoidal, the frequency stays the same. Once it undergoes a period doubling bifurcation at r_2 , two frequencies can be found in the same system, and it is also time dependent. 17
- 2.9 The progression of a system going to chaos. Whether system goes to chaos depends heavily on the initial parameters. In a), it starts out as a single tracing as the initial parameters are set. In b), the system undergoes a period doubling bifurcation, and another tracing appears. In c), they system period double bifurcates again and four tracings exist. in d), the system period double bifurcates so many times that it goes to a chaotic state, and makes it impossible to keep track of the all the tracings. 18
- 3.1 The Langmuir probe circuit diagram with the probe itself located at the very tip. The 400 V DC power supply is used to bias the probe tip. The first voltage (M1) meter is used to obtain the potential of the plasma while the second voltmeter (M2) is used to obtain the voltage across the resistor. We then can use Ohm's Law, $V = IR$, to obtain the current through the Langmuir probe. The idea for this wiring diagram is derived from a paper by Williams [7]. 20
- 3.2 The current - voltage curve using argon. When the bias voltage is very high or very low, the current will eventually saturate, resulting in a flat line. This is not shown in the figure for the electron collection region, but it can be seen for the ion collection region. Adapted from Ref. [1] 21
- 3.3 Our current-voltage curve graph using air. Unlike the I-V curve described in Fig. 3.2, our I-V curve is linear, suggesting that something is wrong when conducting the experiment. The orange triangle indicates the floating potential of the plasma. For this run, the discharge voltage from the high voltage power supply was 699 V, the electrode spacing was 16cm, and the pressure was 11.3 Pa. 22
- 3.4 Our current-voltage curve graph for nitrogen. We were able to obtain a noticeable shift in the current at the V_f . For the parameters, the electrode spacing was 39 cm, the pressure was 114 Pa, and the discharge voltage was 1601 V. 23

| | | |
|-----|---|----|
| 3.5 | The I-V curves of multiple test run using nitrogen with one test run using air using the same parameters as nitrogen. This shows that pressure does have an effect on whether we can obtain the I - V curve if we use a high enough discharge voltage. For the parameters, the discharge voltage was 1601 V, the electrode spacing was 36 cm, and the pressure was 114 Pa. | 24 |
| 3.6 | A graph of the Paschen curve with the raw data and best curve fit plotted with the pressure-distance. For the curve fit parameters, $A = 3800 \text{ Torr}^{-1} \text{ m}^{-1}$, $B = 42787 \text{ V/Torr/m}$, and $\gamma = 0.00432$. The standard deviation of A is $5968 \text{ Torr}^{-1} \text{ m}^{-1}$. The standard deviation of B is $2.43 \times 10^8 \text{ V/Torr/m}$. The standard deviation for γ is 1.34×10^6 | 26 |
| 3.7 | The spectral lines of the plasma using nitrogen. The exposure time was 514.3 ms. It shows the relative intensities of the wavelengths in the plasma. Due to the plasma being composed of molecular nitrogen, there can be other spectral lines appearing that are not the same for atomic nitrogen. | 27 |
| 3.8 | The spectral lines of the plasma using air. The exposure time was 507.2 ms. The graph shows the relative intensities of the wavelengths emitted by the plasma. Despite using different exposure times, resulting in greater peaks, the same wavelengths appear with the added addition of other spectral lines not present in nitrogen such as at 262 nm. | 28 |
| 4.1 | A graph showing the natural log of the current as bias voltage increases for all three time trials for nitrogen. Very near V_f , which is the blue horizontal line, the slope of the curve should be linear, so the electron temperature can be estimated. | 30 |
| 5.1 | The spectral lines of nitrogen provide by the PLASUS Spectral line program. It does not look as if the lines we measured line up with the PLASUS's lines for nitrogen. The majority of the information and functions were locked out because we used a demo version. The full version cost almost 1000 dollars. Retrieved from [13]. | 32 |

1 Introduction

This section describes the general understanding of plasma and the waves present in the plasma. We will also describe our reason as to why we are looking into plasma.

1.1 Plasma

Research in space sciences, industrial applications, and nuclear fusion are some of the reasons why plasma physics has become its own field. To be more specific, one of the challenges of creating a plasma is controlling and containing it. One reason why its difficult to contain and control a plasma is due to the instabilities in the plasma for they have proven to be an issue in controlling chaos. Researching and understanding the nature of plasma is necessary to progress more in other areas of physics and industrial applications. However, even after decades of research, there is still a lot about plasma the scientific community does not understand, which explains why the plasma field in physics is still large today.

Plasma is considered to be the fourth state of matter for its unique properties that differ from the other states of matter. Plasma can be found in neon signs at late-night clubs, the fusion that occurs in stars, the lightning that strikes the Earth during a thunderstorm, or even a brief spark that occurs when a charged object discharges when coming near a conductive material.

A Plasma is an ionized gas, meaning it is a gas like oxygen or nitrogen that has lost one or more electrons. The process of a neutral atom losing electrons and no longer being bound to the atomic core is called ionization. However, a gas suddenly having its electrons no longer bound to its atomic core is not a spontaneous reaction. What has to occur is a free electron – a electron that is not bound to any atom – has to gain enough kinetic energy that when it collides into a neutral particle, the energy from the free electron is deposited into the neutral particle, ionizing it to produce an ion and electron. The newly created free electron then goes on and repeats the process again, creating more free electrons

and ions to the point the overall process cascades. This phenomenon is known as the Townsend avalanche. What is unique about the Townsend avalanche is only a fraction of the atoms are required to be ionized to form plasma [1].

For our experiments, we will be creating a plasma inside a glass evacuated, cylindrical tube with an electrode at each end. We then insert two electrodes inside the glass tube and place a high voltage across them to produce a high electric field. The electric field will accelerate already-free electrons inside the tube until they gain a large enough kinetic energy to ionize neutral particles. The electrons then accelerate towards the positively-charged electrode, ionizing more neutral particles on the way. The ions will accelerate towards the negatively-charged electrode, causing them to emit another free electron upon crashing into the negatively-charged electrode if the ion gains enough kinetic energy to carry out a second ionization.

1.2 Plasma waves

Plasma waves can occur in a wide range of frequencies, but when the oscillations inside the plasma are at lower frequencies like 10^7 to 10^5 Hz, they are usually describing ionization waves [2]. Ionization waves are the end results of the instabilities in a low-temperature plasma [3]. At low frequencies, ionization waves appear as modulations in the ion density moving at a constant phase velocity, and when at higher pressures, they transition to a striation, another type of ionization wave [2]. However, what sets ionization waves apart is how the fluctuations affect the light emission as shown in Fig. 1.1.

A variety of waves can exist inside a plasma, and slightest changes in a single parameter can alter their characteristics. Emma Torbert [4] studied frequencies in the ion acoustic wave as a function of voltage and current. Ion acoustic waves are coherent fluctuations in the density of the plasma; they are the "sound" waves for a plasma. During her experiment, she recorded instances of plasma wave characteristics changing drastically as she varied a single parameter. One of these characteristic changes and the main motivation of this thesis is that when the current was changed by a small amount, the frequency was halved. A phenomenon of a frequency halving is called period doubling. However, at lower currents, Torbert continued to witness these period doubling bifurcations before she concluded that what she saw was Feigenbaum's route to chaos or period doubling cascade to chaos. Period doubling route to chaos is when a system period double bifurcates many times that the overall system becomes aperiodic, and it becomes difficult to keep track of the system. The period doubling occurring in a plasma system is important because period doubling can occur in a variety of other physical systems. Chaos is a term used to describe a system becoming aperiodic, which is best visually described by Fig. ?? and will be explained more in the

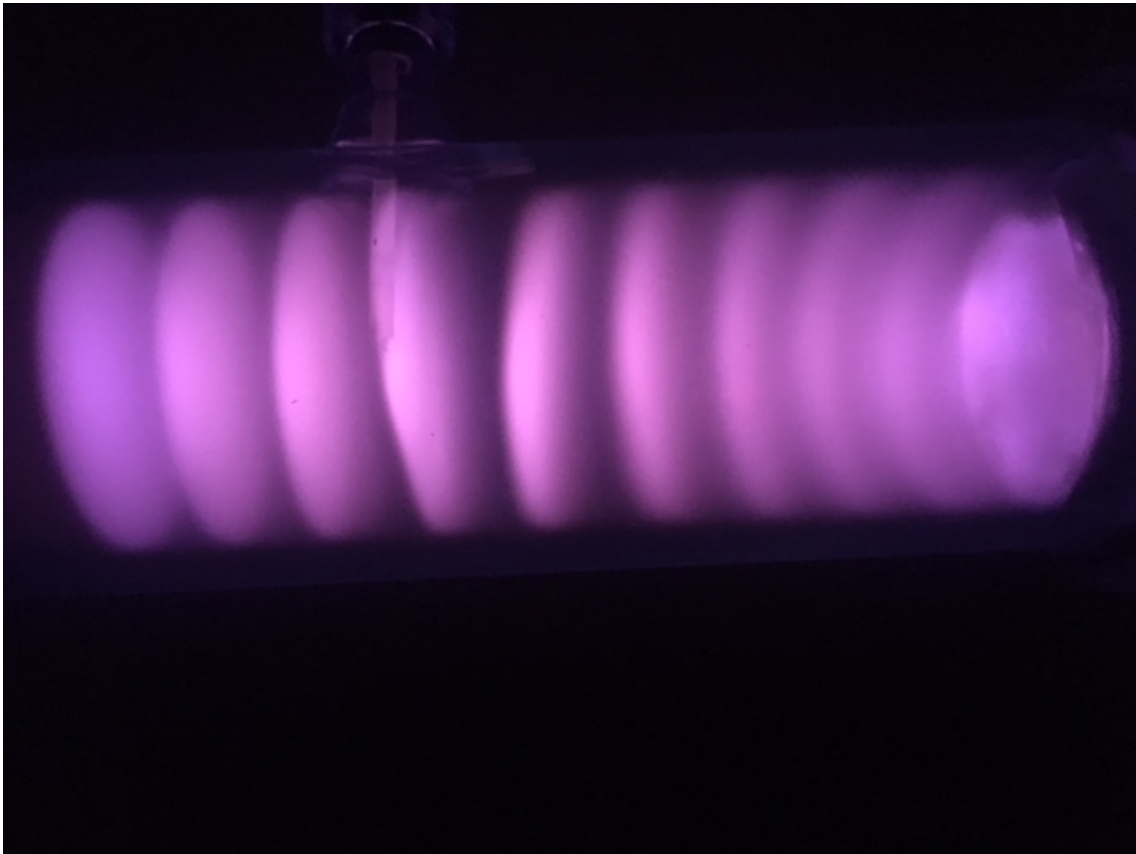


Figure 1.1: A picture of standing striation waves near the positively charged electrode with a probe inserted in the tube.

following chapter. What our experiment focuses on is picking up where Torbert left off and determine why certain plasma waves period double cascade to chaos given the initial conditions. Before we can start understanding why plasma waves go to chaos, we first run some diagnostic test with our plasma tube setup to find the electron temperature and measure the Paschen curve.

The rest of the thesis is organized as follows: Chapter 2 describes necessary background information of Paschen's Law, probe theory, and period doubling, Chapter 3 describes our experimental setup along with our diagnostic testing results. Chapter 4 describes the results of our data with brief explanations on how we obtained those results. Chapter 5 discusses our thoughts about the results and explains more about what could have been improved or done differently to obtain better results.

2 Background Information

In this chapter, we will be discussing first how the electron gains kinetic energy, followed by the relationship the pressure and distance inside the discharge tube with the voltage necessary to achieve a plasma. We will also discuss how a Langmuir probe works in our experiments and follow with an explanation of period doubling and a brief introduction to non-linear dynamics.

In order for a neutral particle to be ionized through electron impact, an electron has to gain enough kinetic energy to strip away electrons. The kinetic energy for a particle is given by

$$K = \frac{1}{2}mv^2, \quad (2.1)$$

where m is the mass of the particle and v is its velocity. Taking hydrogen for example, the amount of energy required to strip away an electron is 13.6 eV. Taking the mass of an electron and converting from electron volts to joules, and taking Eq. 2.1, we can determine the velocity required to obtain the required energy to ionize an hydrogen atom as

$$v = \sqrt{\frac{2K}{m}}. \quad (2.2)$$

Doing the calculation will reveal that the velocity required to ionize a hydrogen atom is 218277 m/s. However, most of the time, particles are unable to reach such speeds because the atmosphere around is filled with millions of particles, so the electron will collide into a particle before reaching an ionizing velocity. The average distance in which a particle travels before colliding with another particle is known as the mean free path length, which is given by

$$\lambda = \sqrt{\frac{k_B T}{\sigma P}}, \quad (2.3)$$

where k_b is the Boltzmann's constant, T is the temperature of the particle, σ is the scattering cross section, and P is the pressure. In a space in which there is a

pressure of one atmosphere, the free mean path length is too short for any particle to reach an ionizing velocity. The pressure inside of the discharge tube is more suitable for creating plasma because very low pressures can be obtained, helping to increase the mean free path length and giving the particles the space needed to accelerate to higher speeds and achieve ionizing velocities.

Once an electron reaches the velocity necessary to ionize neutral particles upon colliding, a free electron is released and allowed to repeat the process again of ionizing another neutral particle to the point where cascading occurs, a process called the Townsend Avalanche. However, the Townsend Avalanche cannot keep the plasma inside the tube for long for a certain amount of ions have to be produced to sustain the plasma. The only way the plasma can sustain itself is if the electron loss and the electron gain are equal, which will be described more in the next section.

2.1 Paschen Law

Paschen's law is an equation that describes the voltage necessary to induce a plasma inside a glow discharge tube as a function of pressure and electrode spacing. To better understand Paschen's Law, it is imperative to understand what is taking place in the plasma during the Townsend Avalanche. As stated previously, the Townsend avalanche occurs when a free electron gains enough kinetic energy to ionize a neutral particle by way of collisions, only for the newly freed electrons to produce more ions via the same process and begin to cascade [1]. The number of electrons N_e and ions N_i as a result to the Townsend avalanche is given by the equations,

$$N_e = e^{\alpha x}, \quad (2.4)$$

and

$$N_i = e^{\alpha x} - 1, \quad (2.5)$$

where x is the distance away from the cathode, the negatively-charged electrode, and α is the rate of ionization rate per unit length [5]. The α in the Eq. 2.4 and 2.5 is also known as the first Townsend coefficient [5], which varies depending on the gas.

However, the ions can also yield another electron. Those ions can accelerate in the direction of the electric field and strike the cathode, possibly ionizing once more to yield another electron. The probability for an ion to emit a second electron at the cathode's location is described by the second Townsend coefficient γ . Its value is dependent on a variety of factors, including the gas, electrode material, and surface conditions. The number of electrons produced from this secondary ionization is given by the equation

$$N_{e_{sec}} = \gamma N_i = \gamma(e^{\alpha x} - 1)[5]. \quad (2.6)$$

A plasma can only sustain itself if after the first electron emission, there are one or more electron emissions to sustain the discharge. With this in mind, $N_{e_{sec}}$ has to equal 1 if the plasma is to sustain itself [5].

The following will be a derivation for Paschen Law given by Dominguez [6]. As previously discussed, α describes the ionization rate per unit length, and it will be used to describe the electron current density, The electron current density is the amount of current flowing through a given area. This is a baseline equation that will eventually help us derive the Paschen curve equation. $\Gamma_e(x)$ is given by

$$d\Gamma_e(x) = \alpha\Gamma_e(x)dx. \quad (2.7)$$

If integrated from the cathode at $x = 0$ to a point inside the discharge tube, the resulting equation becomes

$$\Gamma_e(x) = \Gamma_e(0)e^{\alpha x}. \quad (2.8)$$

It should be noted that since no current is leaving or entering except through the electrodes, and there is no charge build-up, the continuity equation, which describes that the flow of electrons throughout the tube is constant, results in

$$\Gamma_e(0) = \Gamma_e(d), \quad (2.9)$$

where d the distance the anode is from the cathode. This shows the current density at the cathode is the same as the current density of the anode. If there is a single ion species inside the discharge tube, Eq. 2.9 can be written as

$$\Gamma_e(0) + \Gamma_i(0) = \Gamma_e(d) + \Gamma_i(d). \quad (2.10)$$

where d is the total distance between the two electrodes. Since there are no ions at the anode, $\Gamma_i(d) = 0$, and by substituting Eq. 2.8 into Eq. 2.10 and rearranging it, the resulting equation is therefore

$$\Gamma_i(0) = \Gamma_e(0)(e^{\alpha d} - 1). \quad (2.11)$$

As explained before, as the ion reaches the cathode, there is a probability γ that the ion will release a secondary electron, which is expressed as

$$\Gamma_e(0) = \gamma\Gamma_i(0). \quad (2.12)$$

This shows that the electron current density at the cathode is the same as the ion current density with a factor of γ , showing ions have a probability to ionize

once more if they collide into the cathode at a high velocity. When the secondary emission of the electron is able to sustain the plasma, Eq. 2.12 can be substituted into 2.11, ultimately resulting in

$$\alpha d = \ln\left(1 + \frac{1}{\gamma}\right). \quad (2.13)$$

On average, the particles in the plasma travel a certain distance before they collide with another particle. Since the particle can no longer be compressed, it acts like a perfect sphere, so the volume it occupies is $1/n$, where n is the neutral density. In this instance, the cross section for this collision is σ , which is πr_n^2 , where r_n is the radius of the neutral particle. Looking at the particle in two dimensions, it looks like a circle, so the electron has an area that could collide with neutral particles. Altogether, the volume swept out by a neutral particle before a collision is $\sigma\lambda$ since by multiplying an area with a distance yields a volume. Since a neutral gas follows the ideal gas law of $P = K_B n T$, the mean free path is derived once more as seen in Eq. 2.3. Figure 2.1 shows the volume a traveling particle takes up.

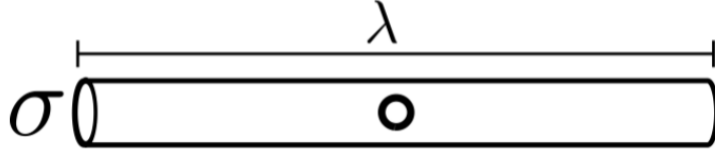


Figure 2.1: The volume a single particle takes up as it moves through the tube before it collides. Adapted from Ref. [6].

The electrons will travel a distance Δ with some electrons colliding with neutral particles during the process, losing some electrons from the $\Gamma_{e_{free}}$, where $\Gamma_{e_{free}}$ is the electron current density for unbound electrons, the free electron current density as seen in Fig. 2.2,. Therefore, we take Dominguez's definition in that λ is also the rate of collision, the solution to the differential equation $\Gamma_{e_{free}}$ is given as

$$\frac{\Gamma_{e_{free}}(x_0 + \Delta)}{\Gamma_{e_{free}}(x_0)} = e^{-\Delta/\lambda}. \quad (2.14)$$

Because the right hand side of Eq. 2.14 is independent of x_0 at any point, the probability for an electron to travel a distance Δ is given by

$$P(\text{distance traveled} \geq \Delta) = e^{-\Delta/\lambda}. \quad (2.15)$$

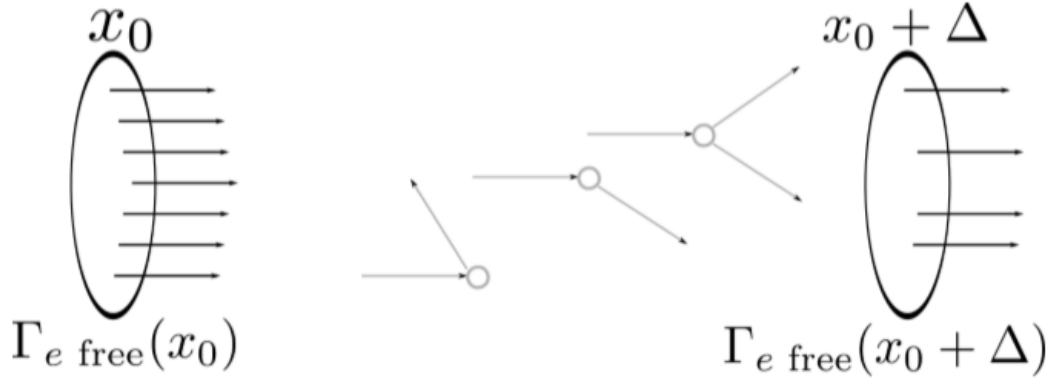


Figure 2.2: A specific section of the tube where the electrons start at x_0 and travel a distance Δ . It also shows some of the electrons are unable to reach the final distance $x_0 + \Delta$ as they collide prematurely. Adapted from Ref. [6].

Looking at α , if all the collisions resulted in ionization, then $\alpha = \frac{1}{\lambda}$, but only a proportion of the electrons that have the energy necessary to ionize the neutral particle, U_I , will cause ionization. Therefore,

$$\alpha = \frac{P(\text{electrons with energy} \geq U_I)}{\lambda}. \quad (2.16)$$

Because the electrons are accelerating through the electric field E , λ_1 is the distance the electron travels in order to gain energy to ionize a particle. This can be written as

$$U_I = eE\lambda_1, \quad (2.17)$$

or

$$\lambda_1 = \frac{U_I d}{Ve}, \quad (2.18)$$

where V is the voltage, d is the distance between the electrodes with both values coming from the fact the electric field $E = \frac{V}{d}$, and e is the charge of the electron. With this, α can be rewritten as

$$\alpha = \frac{e^{-\frac{\lambda_1}{\lambda}}}{\lambda} \quad (2.19)$$

where Eq. 2.15 has been used. If both sides of Eq 2.19 are multiplied by d , we obtain

$$\alpha d = \frac{e^{-\frac{\lambda_1}{\lambda}}}{\lambda} d. \quad (2.20)$$

If we substitute Eq. 2.13 in for αd , Eq. 2.18 for λ_1 , and Eq. 2.3 for λ , the mean free path length, these substitutions result in

$$\ln\left(1 + \frac{1}{\gamma}\right) = \frac{d}{k_b T / \sigma P} e^{-(U_I d / eV) / (k_b T / \sigma P)}. \quad (2.21)$$

After reorganization of the terms by grouping some of them into new terms, it results in

$$\ln\left(1 + \frac{1}{\gamma}\right) = \frac{\sigma}{k_b T} (Pd) e^{-(U_I \sigma / e k_B T) / (Pd / V)} \quad (2.22)$$

so that,

$$\ln\left(\ln\left(1 + \frac{1}{\gamma}\right)\right) - \ln(APd) = \frac{BPd}{V} \quad (2.23)$$

where $A = \sigma / k_B T$ and $B = U_I \sigma / e k_B T$. With all that, the V in the equation becomes the breakdown voltage V_B . We then arrive at the final form of Paschen's law, which is

$$V_B = \frac{BPd}{\ln(APd) - \ln\left(\ln\left(1 + \frac{1}{\gamma}\right)\right)}. \quad (2.24)$$

Figure 2.3 shows the plot of the final form of Paschen's law. If Pd is large, the electrons would collide too much to achieve the necessary energy to ionize the gas particles inside the tube, meaning that the breakdown voltage would need to increase. If Pd is too small, the electrons would not collide with anything other than the cathode at the end, only emitting one electron and secondary emission would not be possible— λ would be big compared to the distance d of the discharge tube.

2.2 Probe Theory

Generally, when it comes to learning more about the properties of a plasma, the best measurement tool available is the Langmuir probe. A Langmuir probe can measure many characteristics of a plasma such as electron and ion densities and the potential of a plasma, but we are more interested in learning more about the electron temperature. In thermodynamics, temperature is related to the average kinetic energy of a gas. The reason for learning the electron temperature is because we want to understand the energies involved in a cold plasma and ensure that our plasma discharge tube setup is functioning, which we will discuss more in Chapter 3.

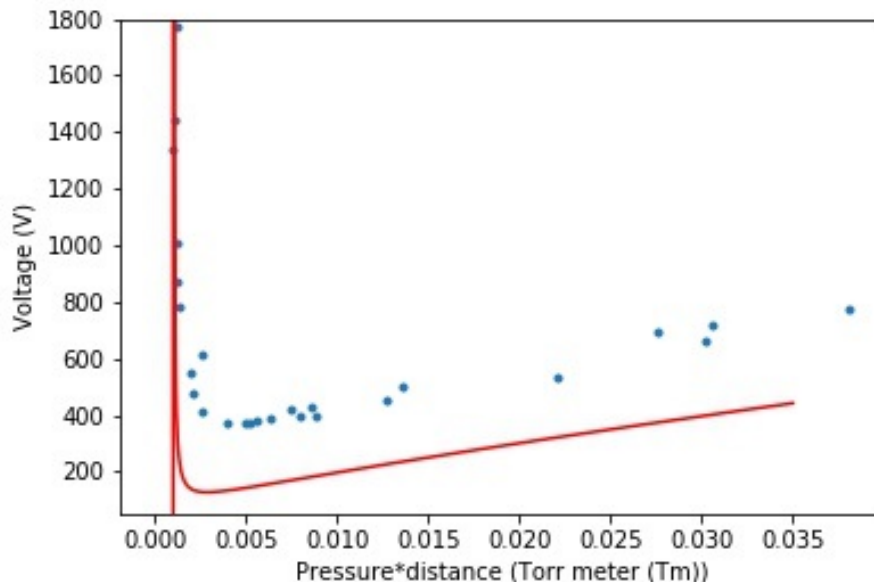


Figure 2.3: Paschen's Law allows us to calculate the V_B as a function of electrode spacing and pressure. The actual points represents the data taken and the curve represents the best-curve fit. We worked with the parameters to make the best fit possible, and the graph is the best fit.

The simplest Langmuir probe construction consists of any conductive material in a specific geometrical shape (planar, cylindrical, spherical), but usually refractive metals – metals that are resilient against heat and wear – like tungsten. This metal is then encased in a ceramic-like boron nitride as seen in Fig 2.4 [1]. The tip of the probe is then electrically biased with respect to one of the electrodes with the use of a DC power supply connected to the probe. The probe is used to measure the electron or ion currents and putting a bias onto the tip helps to control the current.

The following explanation is derived from Jerimiah Williams' handout [7] from Wittenburg University about Langmuir probe construction and experiments. A full nipple, which is just a long metal tube, is used as a case to hold the wire inside. Then, two blank flange with holes drilled into them are placed at each end of the full nipple with O-rings in between them to have a secure seal with from the outside atmosphere. One flange has an industrial feedthrough stainless steel tube soldered to one of the brass flanges to feed the tungsten wire through. The other brass flange has a 15A connector soldered to it to work as an adaptor for connecting BNC cables to the probe. Two cast clamps are used to hold the flanges, the O-rings, and the full nipple together.

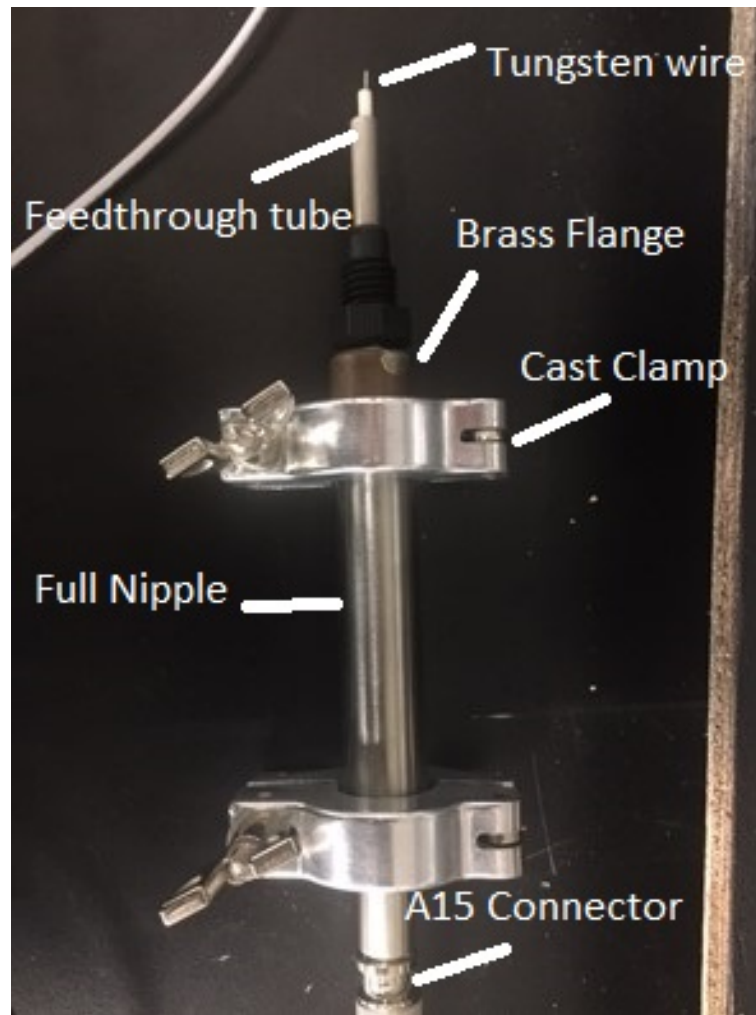


Figure 2.4: A Langmuir probe with a tungsten tip with various parts annotated.

Early users of the Langmuir probe assumed the potential of the plasma at the location of the probe (also called the plasma potential) can be determined by measuring the potential on the probe relative to one of the electrodes. However, that only determines the floating potential V_f and is not the plasma potential V_p [8]. V_f is when the probe inside the plasma has a net current of zero, meaning that the electron current balances out with the ion current, so the potential will rise and fall in order to maintain the zero net current. The reason why V_f is smaller than V_p is mainly due to the electrons. Since the electrons are 2000 times lighter than the ions, they travel at faster speeds and typically reach the probe before the ions could. As the electrons collect at the probe and because a net current on a floating probe must be zero, the potential drifts to the negative side relative to the plasma potential. As the probe becomes more negative due to electrons being faster, electrons start to become repelled, and ions start to be attracted,

thus making V_f slightly smaller than V_p to keep a floating probe's net current zero [8].

A bias potential on the probe that is higher than V_f will cause the tip to be positively charged, attracting electrons to obtain the electron current. A bias voltage that is lower than V_f will cause the tip to be negatively charged, attracting ions and repelling electrons, effectively recording the ion current. In both cases, whatever the potential is on the probe, the surrounding electrons and ions will space themselves out to limit the effect the probe's potential has on the bulk potential in the plasma [8]. For a negatively biased electrode, the shielding distance of the potential disturbance is known as Debye length, and it is given by

$$\lambda_{De} = \left(\frac{\epsilon_0 k T_e}{e^2 n_e} \right)^{\frac{1}{2}}, \quad (2.25)$$

where ϵ_0 is the permittivity of free space, T_e is the electron temperature, e is the charge of the electron, and n_e is the electron density [8].

The following calculations are from Merlino [8] that describes the ion and electron current on a Langmuir probe. For a Maxwellian ion velocity distribution with a dependence on the ion temperature T_i , the ion current $I_i(V_b)$, and bias potential V_b is given by

$$I_i(V_b) = -I_{is} e^{e(V_p - V_b)/kT_i} \quad \text{for } V_b \geq V_p \quad (2.26)$$

or

$$I_i(V_b) = -I_{is} \quad \text{for } V_b < V_p \quad (2.27)$$

where I_{is} is given by the equation

$$I_{is} = \frac{1}{4} e n_i v_{i,th} A_{probe} \quad (2.28)$$

where $v_{i,th} = \sqrt{8kT_i/\pi m_i}$ is the ion thermal speed, m_i is the mass of the ion, n_i is the ion density, and A_{probe} is the probe collecting area. These equations are describing the current through the probe as a certain biased voltage V_b . For an electron, the electron current $I_e(V_b)$ at V_b is given by

$$I_e(V_b) = -I_{es} e^{e(V_p - V_b)/kT_e} \quad \text{for } V_b \geq V_p \quad (2.29)$$

or

$$I_e(V_b) = -I_{es} \quad \text{for } V_b < V_p \quad (2.30)$$

where I_{es} is given by the equation

$$I_{es} = \frac{1}{4} e n_e v_{e,th} A_{probe}, \quad (2.31)$$

where $v_{e,th} = \sqrt{8kT_e/\pi m_e}$ is the electron thermal speed, n_e is the electron density, and m_e is the mass of an electron. Like the current for the ion, this also describes the current through the probe but for electrons instead of ions. When we are at V_f , the net current through the probe is 0. we can then set Eq. 2.27 and Eq. 2.30 equal to each other, becoming,

$$I_{es}e^{e(V_p-V_b)/kT_e} = I_{is}, \quad (2.32)$$

when V_b is equal to V_p . By isolating V_p and having $\frac{I_{is}}{I_{es}} = \frac{2m_i}{\pi m_e}$, we obtain

$$V_p = V_f + \frac{kT_e}{2} \ln \frac{2m_i}{\pi m_e}, \quad (2.33)$$

and this is important because it allows us to measure the electron temperature. Since we do not know what V_p is, we would have two unknowns. However, according to Wissel [1], because the region near V_f is exponential. As a result, the average electron temperature depends on the slope of the current versus voltage relationship, which is

$$kT_e = \frac{dV}{d \ln I}, \quad (2.34)$$

where dV is the change in voltage and $d \ln I$ is the change in natural log of the current. Taking the natural log of the region above V_f where it is exponentially increasing will result in a linear slope near V_f .

2.3 Period Doubling

There are instances when a periodic system undergoes a change, resulting in two frequencies now appearing as seen in Fig. 2.5. This is known as a period doubling bifurcation. However, before discussing period doubling, it is useful to discuss what bifurcations are in the field of nonlinear dynamics because a plasma is considered to be a non-linear system. A bifurcation is any qualitative change in dynamic when a single parameter is varied [9].

A qualitative example of a bifurcation can be a steel beam holding up a weight as seen in Fig 2.6. By putting a light weight on top of a beam, nothing significant will occur because the beam can withstand the weight of the mass. However, as the mass of the weight is increased, the beam continues to support it until it reaches a critical point where the beam cannot support the weight any more and starts to buckle. The critical point where the beam no longer can support the increasing weight and buckles is called a bifurcation. The system was initially in one state, but upon reaching a critical point, the system changes as a result of

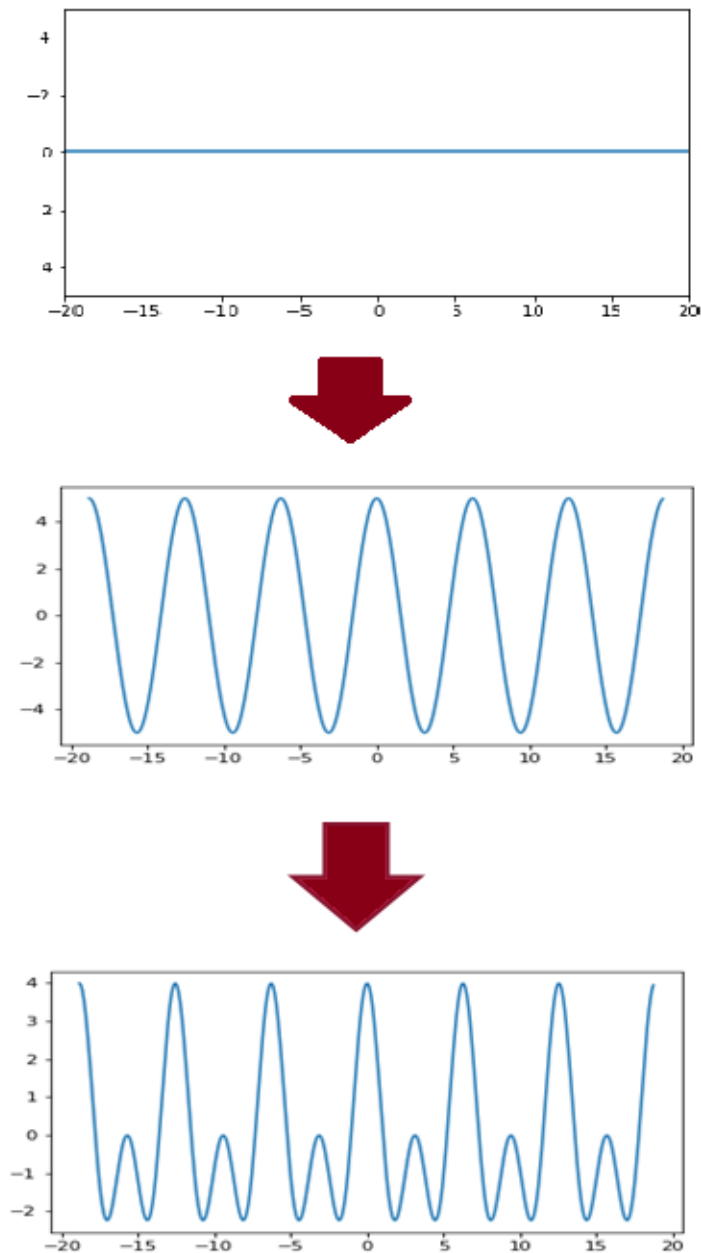


Figure 2.5: a system in which undergoes a Hopf bifurcation which make oscillatory and then undergoes a period doubling bifurcation. After the system undergoes period doubling bifurcation, two frequencies now exist.

varying one parameter. As far as the direction of the bend, it is random since it is equally likely to bend to the right or left.

However, the beam buckling example is not a period doubling bifurcation, but rather a pitchfork bifurcation. At small loads $r < 0$, the beam is straight and stable. When it reaches the critical point $r = 0$, the beam buckles slightly to the right x or to the left $-x$, and as the load increases, the buckling continues, causing for the straight or stable solution to become unstable at $r > 0$ as seen in Fig 2.7. While the pitchfork bifurcation does not change the time dependence of the dynamics, it is possible for a time-independent system to become time-dependent. A system where it goes from time-independent to a time-dependent is called a Hopf bifurcation.

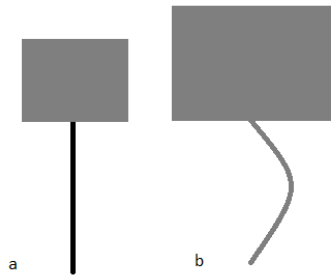


Figure 2.6: An example showing a qualitative bifurcation. a) for small masses the beam can support. b) for large masses the beam cannot support and buckles as a result.

Bifurcations in a plasma also work in the same way in that by varying a parameter (discharge voltage, bias voltage, current, pressure, etc), the plasma can undergo a bifurcation, and more specifically for this thesis, period doubling bifurcations, which in our case is a Hopf bifurcation since it is time-dependent.

Looking at Fig. 2.8, once it undergoes the bifurcation, the system oscillates in the sense that there are two points, and it oscillates between the two points. Once the system period double bifurcates, there is a chance for it to period double bifurcate once more or several more times. This action of a system period doubling bifurcating multiple times will eventually lead the system to chaos. Chaos is a phenomenon in which a system becomes aperiodic and depends on the initial conditions if it becomes aperiodic [9]. In Sprott's discussion [10], she discusses an equation where the system can go to chaos, which is

$$\ddot{x} + a\dot{x} + b\dot{x} \pm (|x| - 1) = 0, \quad (2.35)$$

where a and b are parameters. When $a=0.6$ and $b=1$, the system described by this equation goes to chaos as seen in Fig. 2.9. As a period doubling bifurcation occurs, the tracing takes a new route around. More tracings of the swirl will continue to grow as the system continues eventually going to chaos in time. The

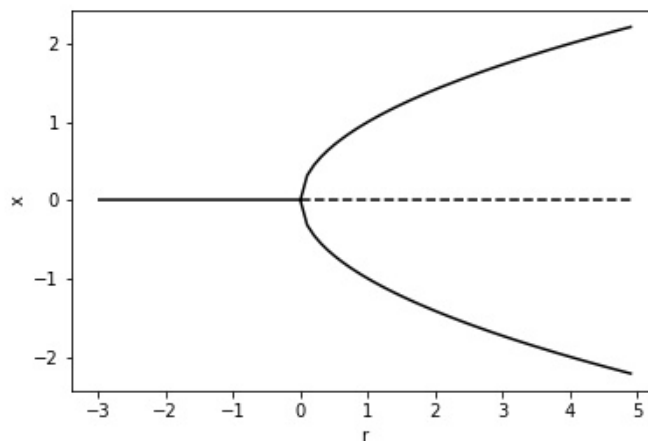


Figure 2.7: A pitchfork bifurcation that splits into two stable and one unstable solutions after undergoing a change at $r = 0$. A solid line represents a stable solution while a dashed line represents an unstable solution.

system starts out as one tracing, and as it period double bifurcates, the number of tracings double. This process occurs so much that it becomes difficult to keep track of the system.

However, systems going to chaos through period doubling bifurcations are not unique to plasma physics because other systems with different physics involved have shown chaos. Examples of this would be dripping water faucets, convection currents, laser systems, and electrical currents. They have all shown that the distance between bifurcations are not random, but governed by an equation known as Feigenbaum's constant δ , which is expressed as

$$\delta = \lim_{i \rightarrow \infty} \frac{r_i - r_{i-1}}{r_{i+1} - r_i}, \quad (2.36)$$

where r_i is the point where the system bifurcates. The literature value for δ is 4.669 [9].

Torbert [4], in her experiment, varies the voltage, current, and pressure one at a time, and as a result, drastically changes the frequency of the plasma. In her experiment, she witnessed her plasma system go to chaos through period doubling bifurcations. While she does provide a possible explanation as to why it is occurring, she did not investigate any further for it wasn't part of her research. We would like to pick up where she left off and explain why the plasma system is going to chaos.

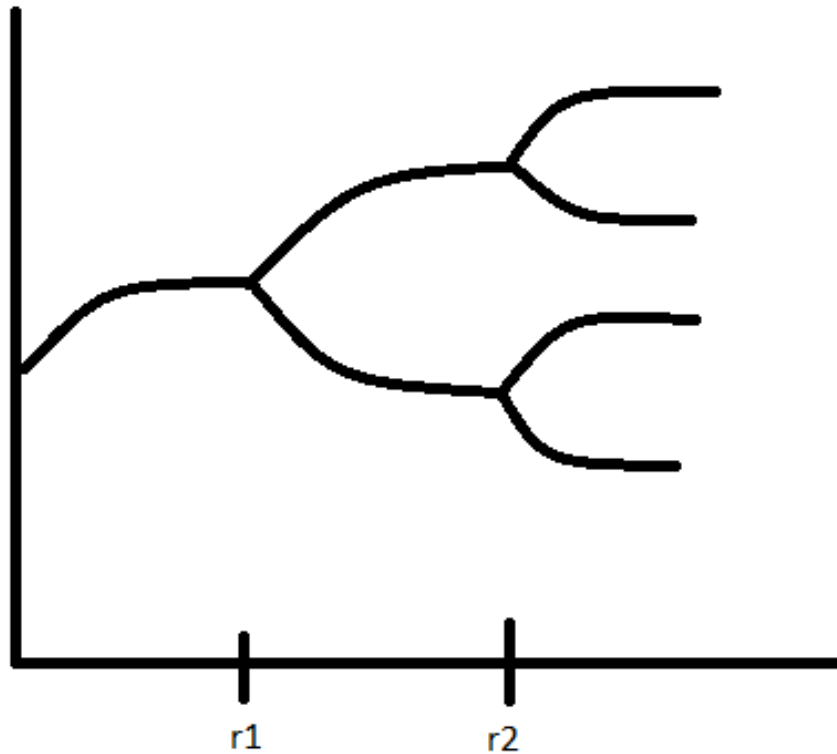


Figure 2.8: A system undergoing a Hopf bifurcation at r_1 and a period doubling bifurcation at r_2 . Once the system goes from a time-independent to a time-dependent system at r_1 , the system oscillates back and forth between points, and the amplitude continues to increase as r increases. While it starts to look less sinusoidal, the frequency stays the same. Once it undergoes a period doubling bifurcation at r_2 , two frequencies can be found in the same system, and it is also time dependent.

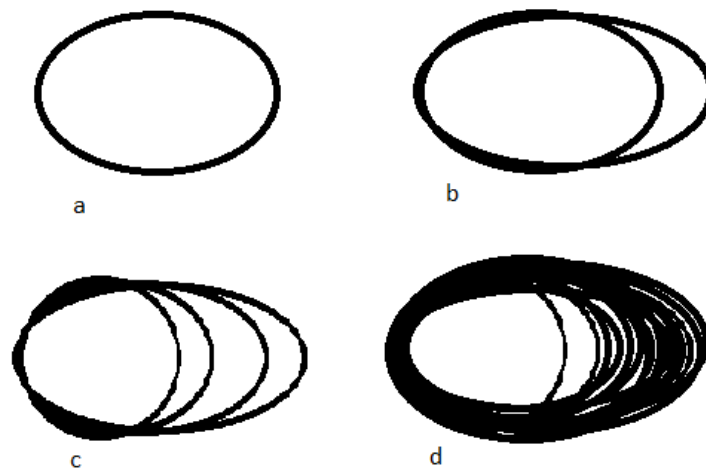


Figure 2.9: The progression of a system going to chaos. Whether system goes to chaos depends heavily on the initial parameters. In a), it starts out as a single tracing as the initial parameters are set. In b), the system undergoes a period doubling bifurcation, and another tracing appears. In c), they system period double bifurcates again and four tracings exist. in d), the system period double bifurcates so many times that it goes to a chaotic state, and makes it impossible to keep track of the all the tracings.

3 Diagnostic Tests

This is the first time a plasma discharge setup has been assembled at Willamette University, so before we moved on to the experimental phase, simple diagnostic tests were performed to ensure our plasma equipment was in working condition by obtaining data like the current-voltage curve and the Paschen curve described in Chapter 2.

3.1 Measuring the $I - V$ curve

One of the diagnostic tests conducted is collecting data of the current-voltage curve for the Langmuir probe inside the tube to estimate the electron temperature described by Eq. 2.33. The method to collect the data is to bias the Langmuir probe by connecting a 400 V DC power supply to the probe. We used air because it is the inexpensive alternative and there are other papers like Dominguez's paper [6] that have obtained the I-V curve using air.

One point of interest for the I-V curve is the floating potential V_f because at that point the net current through the probe is zero. V_f can be obtained by disconnecting the probe from the power supply. This is where the net current is zero, so by placing a positive bias on the tip, we would attract electrons, and placing a negative bias would attract ions. This is important because the speed at which the electrons or ions travel are not the same. Due to the electrons being very light weight compared to the ions, the electrons would travel faster, which can be seen in Fig. 3.2 as the slope after the V_f is steeper. The area around V_f marks a transition point where the curve looks more like an exponential curve before becoming linear as the bias voltage increases. It is this curve that we expect to measure.

We initially biased the probe with a DC-DC converter connected to a 5V DC power supply to sweep across $V_f \pm 100$ volts. The first issue is with the center tap built into the DC-DC converter. With the center tap, it becomes difficult to sweep across zero, so instead of sweep through -100 to 100 volts, we are only able

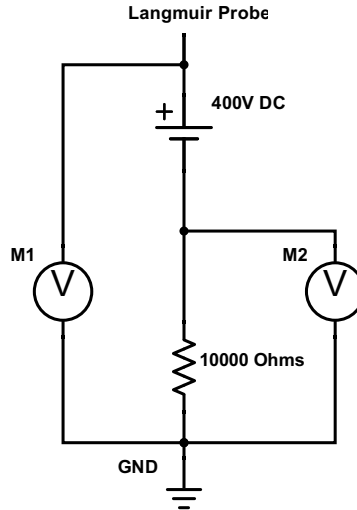


Figure 3.1: The Langmuir probe circuit diagram with the probe itself located at the very tip. The 400 V DC power supply is used to bias the probe tip. The first voltage (M1) meter is used to obtain the potential of the plasma while the second voltmeter (M2) is used to obtain the voltage across the resistor. We then can use Ohm's Law, $V = IR$, to obtain the current through the Langmuir probe. The idea for this wiring diagram is derived from a paper by Williams [7].

to sweep from -100 to 0 volts or 0 to 100 volts. However, the main issue is the inductor built inside of it. It was discovered that when the power supply is turned off, a voltage can still be read. The inductor built inside the DC-DC converter is the issue because there is a noisy current that runs through the inductor. For an inductor, the voltage across an inductor V_L is given by $V_L = -L \frac{dI}{dt}$, where L is the inductance and $\frac{dI}{dt}$ is the change in current with respect to time. In order to have a voltage, the current has to constantly change. Even if the bias power supply is turned off, the plasma causes the inductor to never discharge, so there is always a current running through it. This is a problem because if there is still a voltage across the DC-DC converter despite the power supply being off, it can influence V_f and yield a false floating potential.

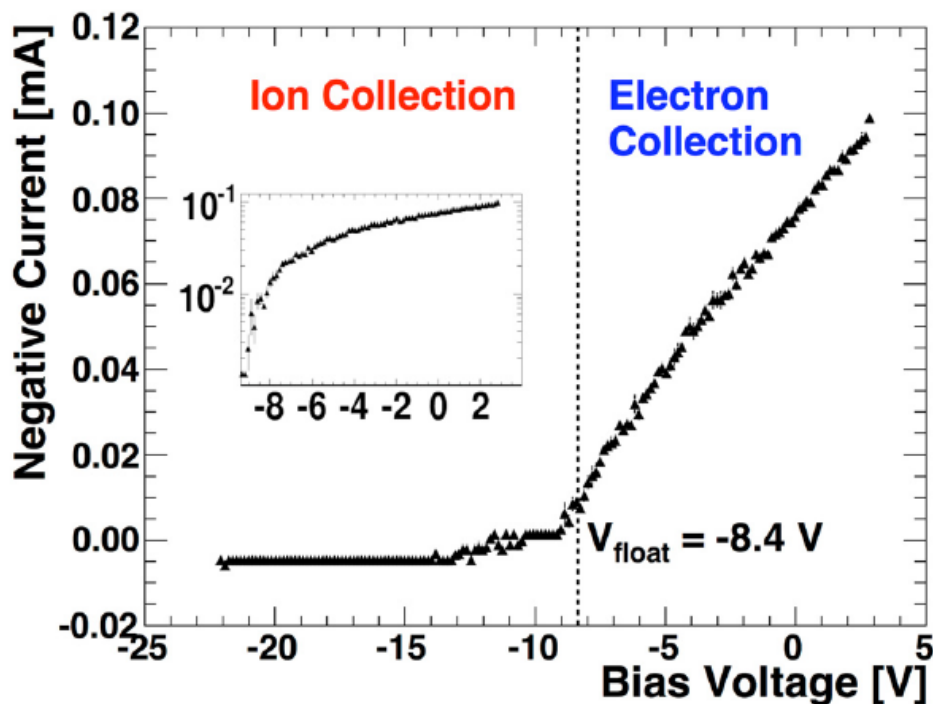


Figure 3.2: The current - voltage curve using argon. When the bias voltage is very high or very low, the current will eventually saturate, resulting in a flat line. This is not shown in the figure for the electron collection region, but it can be seen for the ion collection region. Adapted from Ref. [1]

This issue was solved by replacing the DC-DC converter with a 400 V DC power supply. By hooking the power supply up in replacement to the DC-DC converter, the probe can be biased to gather data about the I-V curve without the fear of a lingering voltage across an inductor.

Upon switching to the power supply, we recreated one of William's circuit [7] for the probe to collect the bias potential as seen in Fig. 3.1. The voltmeter labeled $M1$ is used to measure the bias potential, and the voltmeter labeled $M2$ is used to measure the voltage across the resistor to back out the current. After making the appropriate conversions to volts and milliamps, we plotted our results on a graph as seen in Fig. 3.3. Immediately, our data looks nothing like the I-V curve shown in Fig. 3.2. The first discrepancy is that our curve has a negative current as the bias voltage increases, while the curve in Fig 3.2 has a positive current as the bias voltage increases. This is because our wiring is biased towards ground while the setup used to obtain Fig. 3.2 used a negative power supply to power the cathode and tie the anode to ground, making all their voltage measurements below ground [1].

The bigger issue is our I-V curve is linear throughout the entire range of bias voltages, and we do not have a clear explanation for such an occurrence. We performed this experiment at different pressures, different discharge voltages of the high voltage power supply, and we biased our probe to the positive electrode instead of ground. Other than reversing the entire line to have a negative current as biased voltage on the probe increases, no significant change is observed. Our graphs always look linear.

We reached out to a Professor named Frederick N. Skiff [11] at the University of Iowa private communication and he suggested we use a single species gas because air is not a pure substance like argon or nitrogen for air consists of oxygen, nitrogen, carbon dioxide, etc. [11]. He also said that the water in the air could be affecting our results and can dirty the probe.

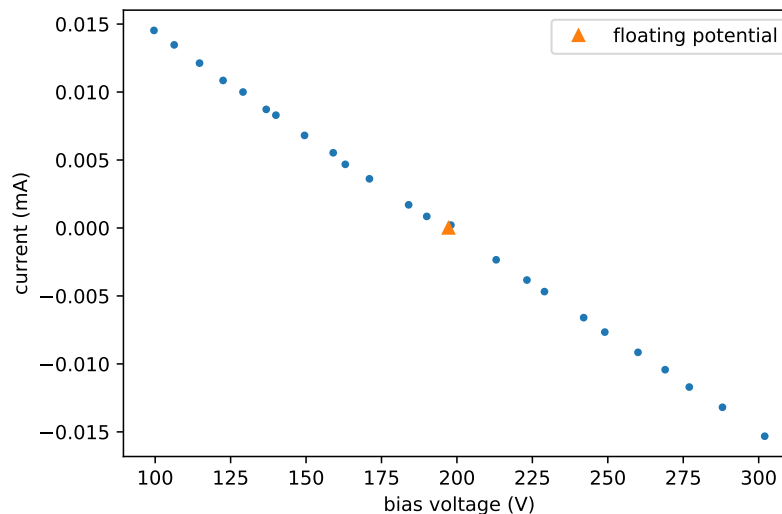


Figure 3.3: Our current-voltage curve graph using air. Unlike the I-V curve described in Fig. 3.2, our I-V curve is linear, suggesting that something is wrong when conducting the experiment. The orange triangle indicates the floating potential of the plasma. For this run, the discharge voltage from the high voltage power supply was 699 V, the electrode spacing was 16cm, and the pressure was 11.3 Pa.

Skiff suggested we switched from using air to nitrogen because working with one species as opposed to working with multiple ones found in air would make it easier to ascertain an I-V curve [11]. After the switch, we ran more I-V curve tests. While most of them were once again straight lines as seen in Fig. 3.3, there were two test runs where we obtained a proper I-V curve we expected to obtain as seen in Fig. 3.4.

We suspected that the reason why some runs worked and other did not is

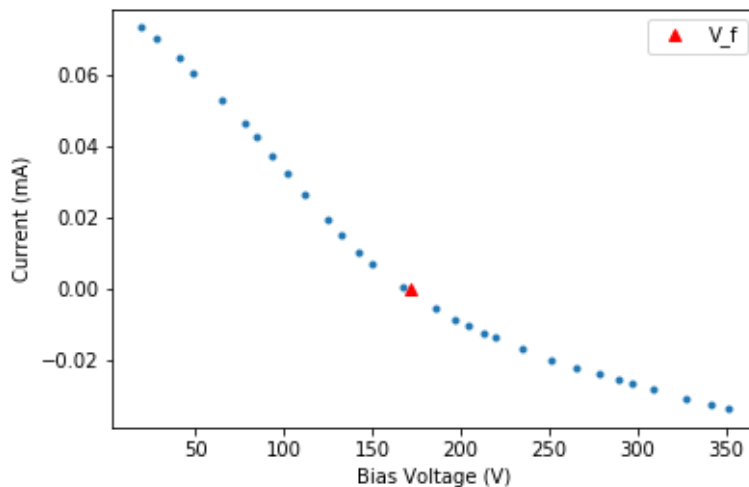


Figure 3.4: Our current-voltage curve graph for nitrogen. We were able to obtain a noticeable shift in the current at the V_f . For the parameters, the electrode spacing was 39 cm, the pressure was 114 Pa, and the discharge voltage was 1601 V.

because while the tube was filling up with nitrogen, the tests were conducted when some air was still inside, thus influencing the results. To confirm this suspicion, we ran three tests where pressure, discharge voltage from the high voltage power supply, electrode spacing, the resistance, and floating potential were constant. The only variable that was changed was when the tests were conducted. One test was conducted immediately after the pressure was stabilized. We then waited for twenty minutes to allow more nitrogen to fill the tube so less air was inside. For the last test, we waited up to an hour for nitrogen to fill up the tube and conducted the test as seen in Fig. 3.5 and where are main data is coming from. However, no matter how much time we waited, all the tests were consistent.

There was still one last suspicion we wanted to test. We suspected that the pressure may have been affecting the IV curve. We decided that using the same parameters listed in Fig. 3.5, we conducted the test once more but with air. As it turns out, we were once again able to obtain the I-V curve for air as seen in Fig 3.5. As we thought, it appears that pressure does play a role in obtaining the I - V curve, even with air. The last test we conducted with air, we were working with pressure between 10 to 30 Pa and only ascertained straight lines. We think that there might be a pressure voltage trade off. If the pressure is very low, we would need to apply a very high voltage, and as the pressure increases, the voltage required to obtain an I-V curve decreases, but if the pressure is too high, then the air inside the discharge tube will not ignite. In other words, there is a sweet

spot between pressure and voltage that we were not hitting when we conducted the test using air as we were working very low pressures.

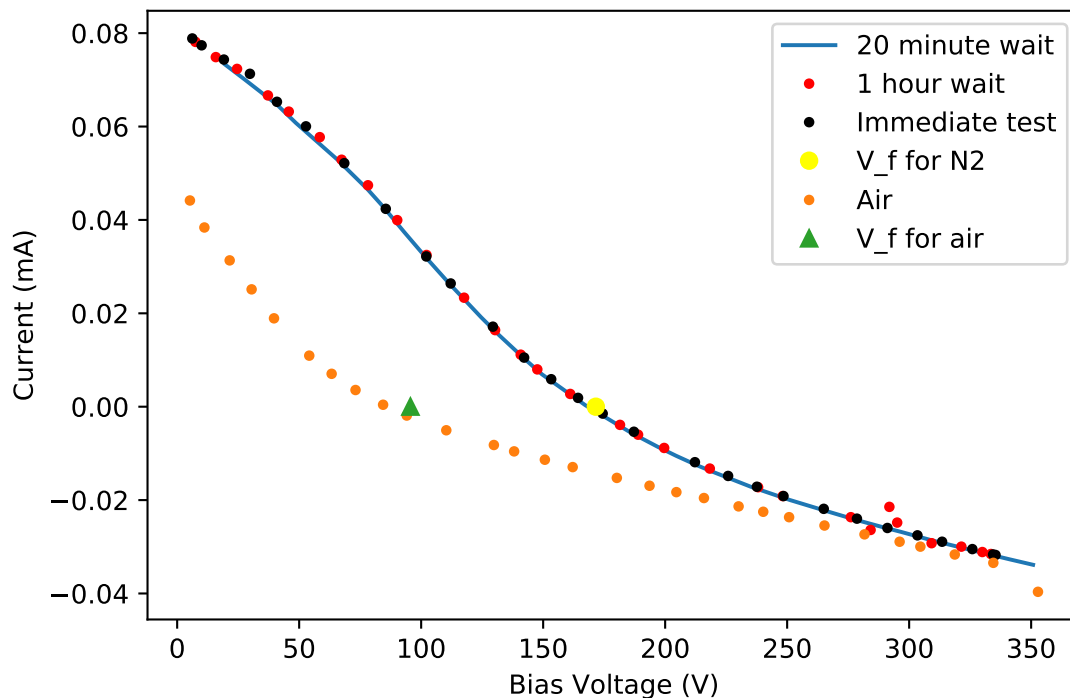


Figure 3.5: The I-V curves of multiple test run using nitrogen with one test run using air using the same parameters as nitrogen. This shows that pressure does have an effect on whether we can obtain the I - V curve if we use a high enough discharge voltage. For the parameters, the discharge voltage was 1601 V, the electrode spacing was 36 cm, and the pressure was 114 Pa.

3.2 Obtaining the Paschen Curve

With many problems in attempting to measure the I-V curve, we switched our focus to ascertain the Paschen curve using air as the gas. This experiment was conducted before learning about the issues of air. As stated previously, air is not a single species as it consist of multiple species. This is important because the Paschen curve equation (Eq. 2.24) uses the second ionization constant γ in the equation, and that describes the probability of an ion releasing another electron. With so many species mixed into air, there are multiple γ 's, and it can be difficult to determine the correct γ for it would be an average of all the *gamma*'s for all

the species. Looking at the derivation provided by Dominguez [6], we chose γ to be 0.02 just for the sake of quickly gathering the Paschen curve.

The general process for measuring the Paschen curve was to first set the electrodes a fixed distance away. We opted to place the electrodes 5 cm apart in order to have the discharge voltage be within 2000 volts, the same voltage as our high voltage power supply. We would then activate the pump to decrease the pressure to a desired value. The high voltage power supply was turned on, and we increased the voltage until the air inside is ignited into a plasma. We recorded the pressure and voltage, turned off the high voltage power supply, and ran the test again another two times. We then took the average of the three discharge voltages. This process is continued for other pressures. Once a sufficient amount of points are taken, we plotted our data. With the points plotted, the Paschen curve can be identified as seen in Fig. 3.6, but in order for us to have the best-fit curve plotted alongside the data points, we used Python's Curve fit function.

The first issue in plotting the best-fit curve is that the resulting curve would look like the Paschen curve, but shifted to the right. This was ameliorated by placing a condition saying one of our fit parameters had to be bigger than a certain value. We did this because as seen in Eq. 2.24, the denominator will eventually equal zero, creating a singularity in the form of an asymptote. Because of this asymptote, the curve fit function would try its best to find a working parameters, but since the equation is non-linear, it would yield curves shifted to the right. This problem was fixed by finding the smallest possible A and setting the denominator in Eq. 2.24 to A . Looking at Fig. 3.6, the smallest pressure-distance point is used by substituting it in for the denominator to find what the lowest possible A . Once the lowest A is known, we set a constraint saying A has to be greater than the previous value found. After putting in several guesses for what the parameters A , B , and γ , the best-fit curve was yielded, which is shown in Fig. 3.6. The values of A and B in Dominguez's derivation were $1500 \text{ Torr}^{-1} \text{ m}^{-1}$ and $36000 \text{ V/Torr/meters}$. They are within one standard deviation; however, the standard deviations are very big as $\sigma_A = 5968 \text{ Torr}^{-1} \text{ m}^{-1}$, $\sigma_B = 2.43^8 \text{ V/Torr/m}$, and $\sigma_\gamma = 0.00432$, and the reason is it is not a good fit. Its clear that the raw data is above the fitted curve. The reason for this is the air inside the discharge tube can become conductive before reaching the discharge voltage, making the curve fit sit below the raw data points [1]. Once we saw the plasma form, we took down the discharge voltage. We did, however, endeavor to find the discharge voltage when the gas becomes conductive before the plasma is formed by placing a multi-meter in series with the two electrodes to see if we can read a current before the plasma was formed. We did this to correct for the downward shift of the best-fit curve. This did not work because once we obtained a measurement on the multi-meter in series with the high voltage power supply, a plasma was already visible.

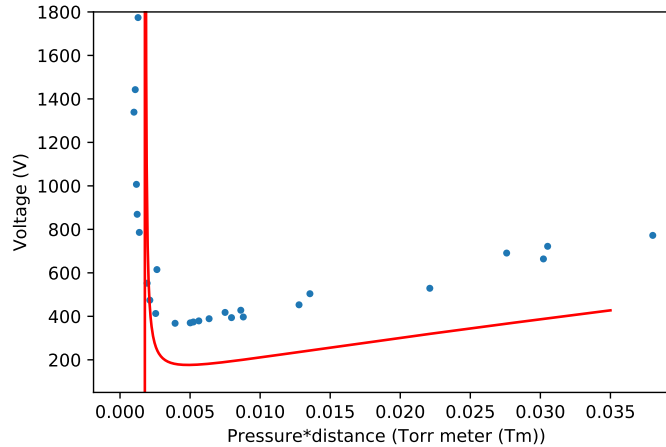


Figure 3.6: A graph of the Paschen curve with the raw data and best curve fit plotted with the pressure-distance. For the curve fit parameters, $A = 3800 \text{ Torr}^{-1} \text{ m}^{-1}$, $B = 42787 \text{ V/Torr/m}$, and $\gamma = 0.00432$. The standard deviation of A is $5968 \text{ Torr}^{-1} \text{ m}^{-1}$. The standard deviation of B is $2.43 \times 10^8 \text{ V/Torr/m}$. The standard deviation for γ is 1.34×10^6

3.3 Spectroscopy

Spectroscopy is the measurement of spectra produced when matter interacts with or gives off electromagnetic radiation. It is another way to measure plasma parameters such as the electron temperature or density. The idea is light is emitted from the atoms once an electron interacts with them. If we assume the electrons interacts with the atoms in the ground state, then the spread of the excited levels depend on the electron energy distribution for if the electron has more energy, it can excite higher atomic levels [1]. We can observe the spectral lines and use them to estimate the electron temperature [1].

The following discussion comes from Wissel's paper [1]. The intensity I_{ik} is proportional to $\frac{hcA_{ki}n_k}{4\pi\lambda_{ki}}$, where h is Planck's constant, c is the speed of light, A_{ik} is the transition probability for spontaneous emission from a state k to a state i , n_k is the population of the excited states. If we assume the Maxwell-Boltzmann distribution, n_k depends on the Boltzmann factor e^{-E_k/kT_e} and the quantum degeneracy factor g_k that describes the number of states with the same energies, where E_k is the upper energy level, k is the Boltzmann constant, and T_e is the electron temperature. Taking the natural log will give a linear function, which is

$$\ln \frac{\lambda_{ki} I_{ki}}{g_K A_{ki}} = \frac{E_k}{kT_e} + C, \quad (3.1)$$

where C is a constant. By plotting points of the upper energy against the natural log, a best-fit, linear slope can be created, and we can derive T_e from it.

Using a Mightex Spectrometer HRS-BD1, we placed an optical fiber against the side of the plasma tube near the positive electrode where the majority of the plasma was forming. Looking at the largest peaks, we took down the wavelengths and relative intensities as seen in Fig. 3.7. The intensities of the wavelengths for air were also taken to compare to nitrogen to see if there are any differences between nitrogen spectral lines and air spectral lines as seen in Fig 3.8. The value A_{ki} can be found on the NIST website [12] for each corresponding wavelength. g_k will be discussed later as we did encounter problems.

Looking at Fig. 3.8, we see spectral lines that are present in air, but not in nitrogen. A line that does appear in air are at 262 nm.

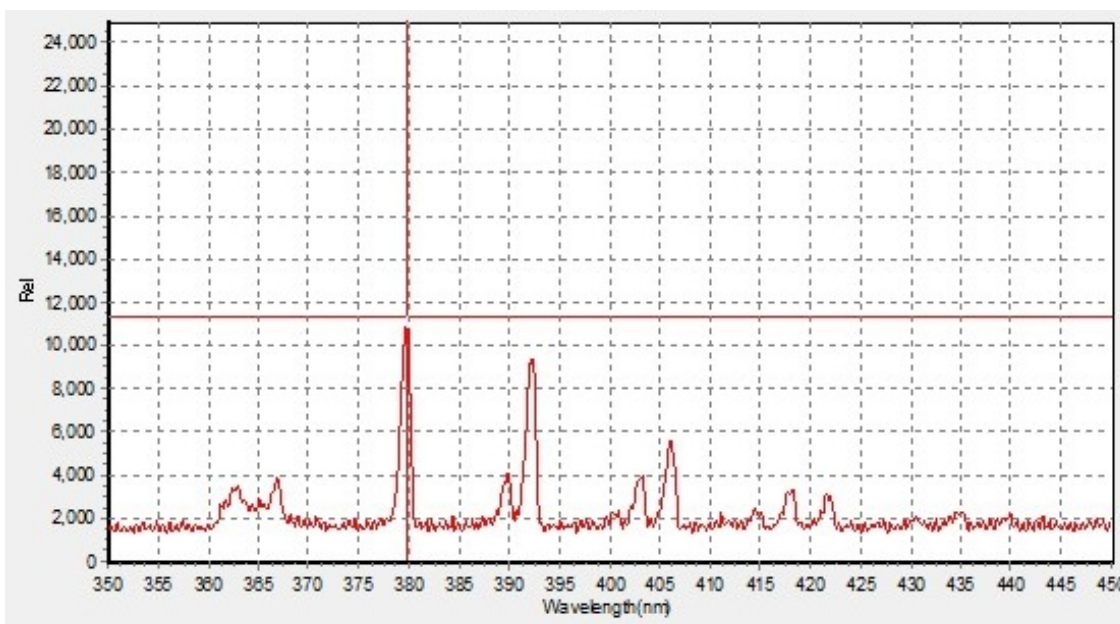


Figure 3.7: The spectral lines of the plasma using nitrogen. The exposure time was 514.3 ms. It shows the relative intensities of the wavelengths in the plasma. Due to the plasma being composed of molecular nitrogen, there can be other spectral lines appearing that are not the same for atomic nitrogen.

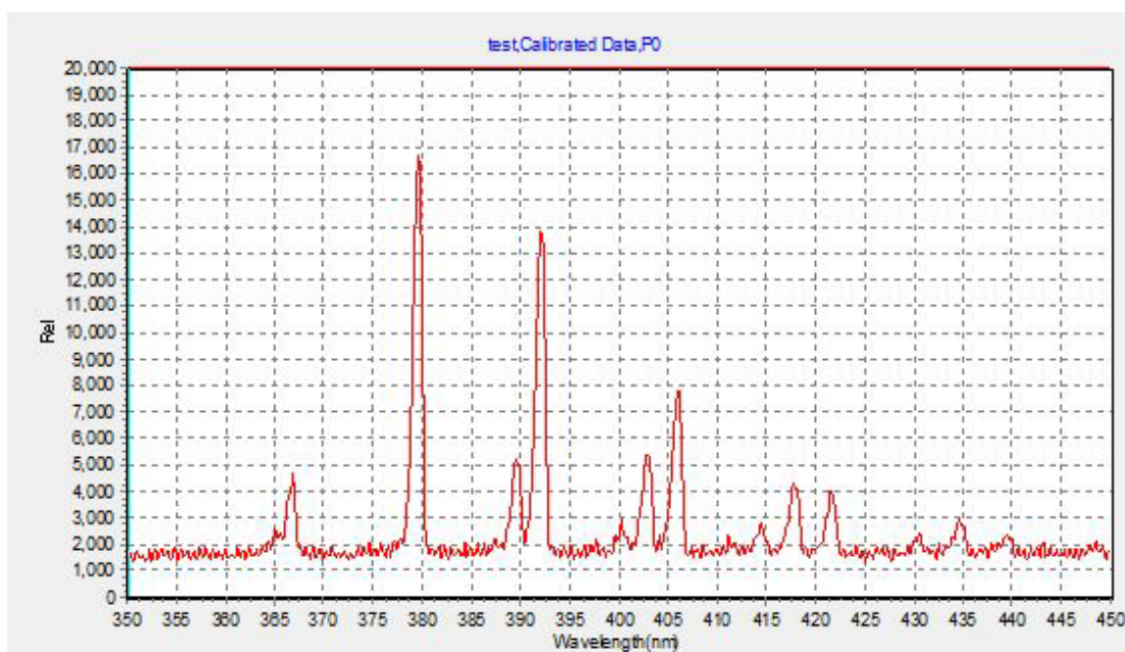


Figure 3.8: The spectral lines of the plasma using air. The exposure time was 507.2 ms. The graph shows the relative intensities of the wavelengths emitted by the plasma. Despite using different exposure times, resulting in greater peaks, the same wavelengths appear with the added addition of other spectral lines not present in nitrogen such as at 262 nm.

4 Results

When it comes to the Paschen curve, we were able to obtain it for air as seen in Fig. 3.6. The best fit curve is below the actual data points, but is to be expected as described in Chapter 3. Our values for A and B are $3800 \pm 5968 \text{ Torr}^{-1} \text{ m}^{-1}$ and $42787 \pm 2.43 \times 10^8 \text{ V/Torr/m}$. While we were able to achieve the Paschen curve, our parameters are questionable because the standard deviations are very large.

What we are more interested in obtaining is the electron temperature through the use of the I-V curve. In spite of having Eq. 2.33 to calculate T_e , we do not know V_p because the voltages read across the voltmeter does not read the plasma potential; it reads the bias we place on it. It is possible to estimate T_e since just above V_f , the curve is increasing exponentially due to the fact the electron distribution is Maxwellian [1]. This is true if we use a negative DC power supply, but since we used positive DC power supply, our circuit is biased towards ground. As a result, our current-voltage curve is a reflection of Wissel's current-voltage curve.

Using Eq. 2.34, we can derive T_e as seen in Fig. 4.1. From the calculation, the electron temperature is 2.87 eV. It is given in eV instead of temperature because energies are more useful than temperature.

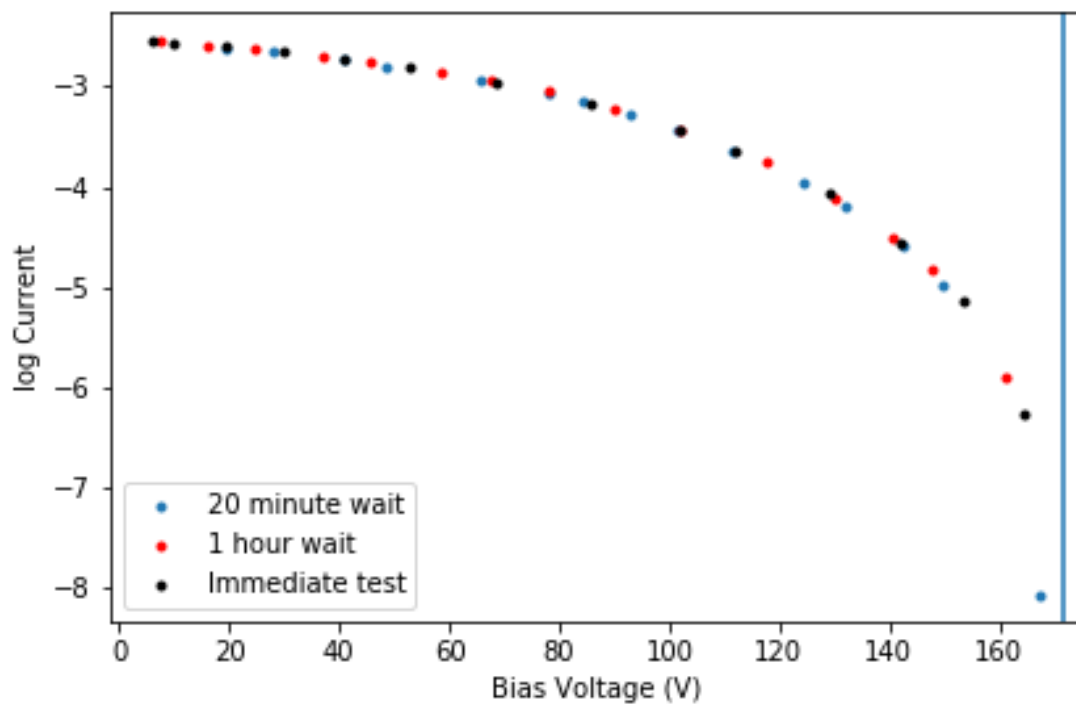


Figure 4.1: A graph showing the natural log of the current as bias voltage increases for all three time trials for nitrogen. Very near V_f , which is the blue horizontal line, the slope of the curve should be linear, so the electron temperature can be estimated.

5 Discussion

There is not a lot of confidence in our electron temperature value because we did not put down an uncertainty. This is because there are not enough points near V_f that follow a linear increase. Looking at Fig. 4.1, the region near V_f should be exponential, so taking the natural log near V_f should yield a linear trend before it starts to curve. However, the region for exponential increase just above V_f is so tight, not enough points were taken in that region to accurately create a best-fit line. As seen in Fig. 4.1, right after the second point, the curve is no longer linear, so as a result, only the first two points after V_f were used to obtain the slope through the rise over run method. The rise is the log current and the run is voltage, so once the value was calculated, we took the inverse to portray $\frac{dV}{d \ln I}$.

A better example showing this linear line near V_f is best shown in Fig. 3.2, where Wissel shows the small window similar to Fig. 4.1. Using the first couple of data points before the curve becomes non-linear is what helped them secure an estimate for the electron temperature gas. For her results, she calculated an electron temperature of 0.75 eV. We are very off from her results.

We were unable to obtain an electron temperature during the spectroscopy due to the nature of nitrogen. Nitrogen is a diatomic molecule, meaning it has more degrees of freedom as opposed to atomic nitrogen. As seen in Fig. 3.7, there are spectral lines that appear that we cannot identify due to the extra degree of freedom as seen in Table 1. Also, looking through the NIST website [12] to see what wavelengths correspond to what energy transition of the electrons in nitrogen, the values we measured correspond to various ions of nitrogen ranging from N^+ and N^{3+} . We expected for N^+ and N^{2+} to be existent due to the first and second Townsend Avalanche, but it would appear that some of the spikes correspond to other nitrogen ions. We did use a program called PLASUS Spectral Line, which is a program that shows the information and spectral lines of elements and molecules [13]. We found a spectral graph of nitrogen as seen in Fig. 5.1. However, it did not look like the lines on the program are lines up with our lines.

Another issue encountered is some of the wavelengths listed on the NIST website did not correspond to the wavelengths we saw, or the wavelengths were not

Table 1: A table of all the wavelengths present in the nitrogen-based plasma. The dashed lines represent data could not be found for those specific wavelengths. The R 's next to the wavelengths means that the wavelength is the Ritz wavelength, which are wavelengths calculated from energy level differences. For all of the wavelengths, we had to take the closest wavelengths listed on the NIST website.

| N Ion | Wavelength (nm) | Observed Intensity (J) | A_{ki} |
|-------|-----------------|------------------------|----------|
| 3 | 367.032 R | 3829 | 4.66e+03 |
| 3 | 379.832 R | 11436 | 1.03e+07 |
| 1 | 389.912 R | 4017 | 2.50e+06 |
| 2 | 392.314 R | 9180 | 7.99e+06 |
| 2 | 403.384 R | 4098 | — |
| — | 406.116 | 5540 | — |
| 2 | 417.739 R | 3141 | — |
| 3 | 421.793 R | 2917 | 1.85e+07 |

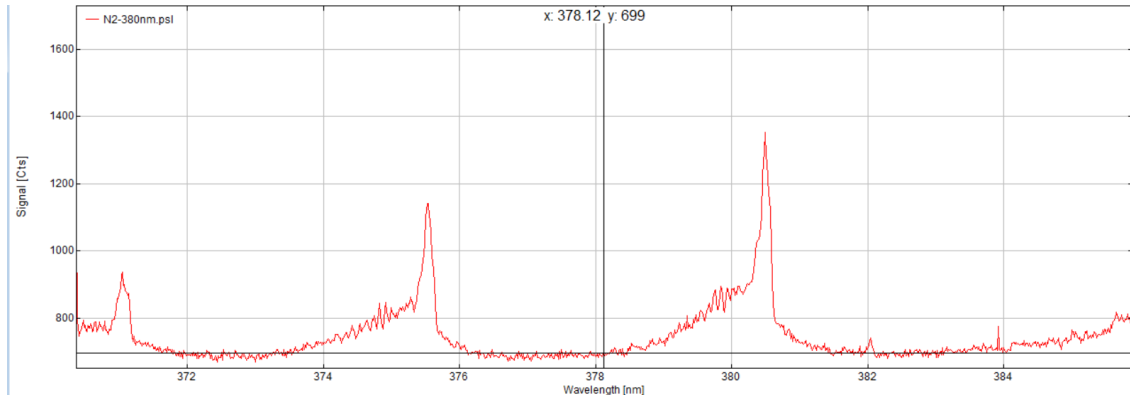


Figure 5.1: The spectral lines of nitrogen provide by the PLASUS Spectral line program. It does not look as if the lines we measured line up with the PLASUS's lines for nitrogen. The majority of the information and functions were locked out because we used a demo version. The full version cost almost 1000 dollars. Retrieved from [13].

listed. We suspect it may be due to the diatomic nature of nitrogen. However, the biggest issue is g_K for we could not find that value for nitrogen or its ions, and due to limited time, we were unable to find any g_k values before the completion of this thesis. As a result, we could not accurately plot down energies, and no T_e could be recorded using spectroscopy.

As a recommendation to anyone who wishes to conduct these tests, it would be best to use a noble gas like argon like many others before us because a lot of the data of argon is well known. Using a well-documented gas to conduct diagnostic test is more efficient and provides a way for checking accepted literature values

against experiments.

Due to the difficulty of conducting the various diagnostic tests, we were unable to move past the diagnostic phase and conduct any experiments involving period doubling bifurcations. However, since we now know our glow discharge apparatus does work, we have finished the groundwork so if future students want to conduct experiments with the glow discharge apparatus setup at Willamette University, they can start their experiments knowing the glow discharge apparatus is in working condition.

Bibliography

- [1] S. A. Wissel, A. Zwicker, and S. G. Jerry Ross, “The use of DC glow discharges as undergraduate educational tools,” *American Journal of Physics*, vol. 81, no. 663, 2013.
- [2] M. N. Hirsh and H. J. Oskam, Eds., *Gaseous Electronics*, 1st ed. Academic Press Inc., Cambridge, MA, Aug. 1978, vol. 1.
- [3] A. Dinklage, B. Bruhn, H. Testrich, and C. Wilke, “Hysteresis of ionization waves,” *Plasma of Physics*, vol. 15, 2008.
- [4] E. Torbert, “Discrete modes in the ion acoustic range of frequencies in a glow discharge plasma column,” Princeton University Undergraduate Thesis, 2001.
- [5] T. Y. Slah and T. P. Ivan, “Plasma physics: Paschen curve,” 2010.
- [6] A. Dominguez, “Derivation of the Paschen curve law: ALPhA laboratory immersion,” Jul. 2014. [Online]. Available: https://www.compadre.org/advlabs/bfyii/files/Paschen_derivation.pdf
- [7] J. Williams, “Handout for plasma physics: Plasma probes,” Jun. 2014. [Online]. Available: http://www.compadre.org/advlabs/images/files/LangmuirProbe_handout_2014.pdf
- [8] R. L. Merlino, “Understanding Langmuir probe current-voltage characteristics,” *American Journal of Physics*, vol. 75, 2007.
- [9] S. H. Strogatz, *Nonlinear Dynamics and Chaos*. Perseus Books Publishing, New York, NY, 1994.
- [10] J. C. Sprott, “Complex behavior of simple systems,” in *Unifying Themes in Complex Systems*, A. A. Minai and Y. Bar-Yam, Eds. Berlin, Heidelberg: Springer Berlin Heidelberg, 2006, pp. 3–11.
- [11] F. N. Skiff, Private Communication, Feb. 2019.

- [12] Y. R. et al., “NIST atomic spectra database,” National Institute of Standards and Technology, Apr. 2019, <http://physics.nist.gov/asd>.
- [13] PLASUS, “Plasus Spectral line,” Computer Program, <https://www.plasus.de/index.php?page=start&lang=en>.